Proceedings World Geothermal Congress 2020+1
Reykjavik, Iceland, April - October 2021

Assessment of Fault Permeability Using Soil Gases in Palinpinon Geothermal Field, Philippines

Jigo W. Mismanos and Gabriel P. Mendoza

Energy Development Corporation, 38F One Corporate Centre, Julia Vargas cor. Meralco Avenue, Pasig City, Philippines

mismanos.jw@energy.com.ph

Keywords: Palinpinon, soil gases, permeability, radon, thoron

ABSTRACT

Soil gas surveying is a potentially useful method in identifying permeable faults in geothermal fields. Mapping the surface concentrations and flux of soil gases, particularly radon (^{222}Rn), thoron (^{220}Rn), and CO_2 can delineate the structures that serve as reservoir fluid pathways which may be tapped by production wells. In this study, a grid survey was conducted in the South Sogongon and Nasuji sectors of the Palinpinon Geothermal Field to evaluate the permeability of the faults in these areas. Grid measurements were obtained using alpha spectroscopic detectors for the radioactive gases and accumulation chamber with IR detector for soil CO_2 flux. The relationship of soil gases with fault permeability, as reported from well drilling and well-testing, was determined using logistic regression. The logistic regression model identified radon and thoron as the best predictors of fault permeability. Using this model, the high soil gas anomalies corresponding to good permeability identified the NW-SE and NW-SE faults as good candidates for drilling geothermal wells.

1. INTRODUCTION

The Palinpinon Geothermal Field is located in central Philippines (Figure 1). Operating for over 30 years now, Palinpinon is one of the oldest operating geothermal fields in the world. Managing the sustainability of the geothermal resource has been the key to the field's three-decade utilization. An integral part of the upkeep of the field is the drilling of new wells, and its success (i.e., encountering highly permeable and/or productive feed zones with high output) is largely dependent on the geoscientific knowledge that the drilling strategy was based upon. While conventional geologic mapping has been adequate in mapping the permeable fluid-bearing structures since the onset of exploration, other surface investigation methods that can corroborate permeability are also being considered, such as geophysical imaging and soil gas mapping.

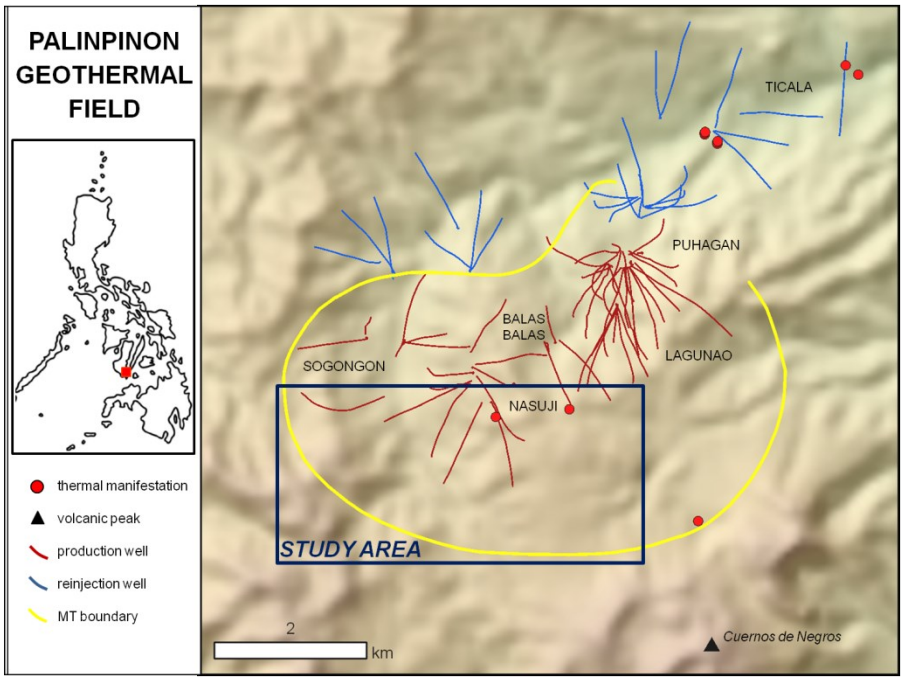

Figure 1: Map of Palinpinon Geothermal Field showing soil gas study area in South Sogongon and Nasuji.

Soil gas surveying, a surface geochemical survey method, has been studied as a potential method in identifying permeable structures in geothermal systems. The method relies on the surface concentrations of soil gases to delineate the permeable structures that serve as pathways for reservoir degassing. Carbon dioxide and radon (^{222}Rn) are typically used for their good tracer qualities.

In geothermal systems, carbon dioxide (CO_2) generally constitutes 80% of all gases excluding steam (Mahon, McDowell, & Finlayson, 1980). Elevated carbon dioxide fluxes in soil have been measured above geothermal resources, typically at hot grounds and faults/structures (Chiodini, Cioni, Guidi, Raco, & Marini, 1998; Klusman, Moore, & LeRoy, 2000) but anomalous CO_2 fluxes have also been encountered above main upflow zones (Werner & Cardellini, 2006).

Radon is a radioactive noble gas formed from the decay of uranium. ^{222}Rn (radon), the most abundant isotope, has a half-life of only 3.8 days. Another isotope of radon, ^{220}Rn (thoron), has a much shorter half-life of only 55.6 seconds. Rapid extraction of large amounts of radon from deeper origins is generally made possible by convection (Cox, 1980; Witcher, 1991). Permeable vertical conduits such as faults and fractures provide pathways of rapid bulk transport from depth to surface, where they can occur at levels higher than background (Voltattorni & Lombardi, 2010).

In soil gas surveys conducted in Bac-Man and Mahanagdong geothermal fields, high soil gas concentration anomalies were observed above traces of faults where wells encountered good permeability (Mismanos & Vasquez, 2015; Vasquez, Abecia, & Cariaga, 2015). This observed relationship was seen as basis in identifying and delineating potentially permeable structures that can be targeted for drilling exploration and/or make-up and replacement (M&R) wells. By mapping the anomalous concentrations of radon, thoron, and CO_2 flux, this study aims to investigate the permeability of structures in the South Sogongon & Nasuji Sectors of Palinpinon and determine their viability as future drilling targets.

2. METHODOLOGY

Soil gas surveys were conducted in the South Sogongon and Nasuji sectors of Palinpinon. Measurements were taken along fault traces and blocks. Each station is spaced roughly 150 m apart. Radon and thoron in soil gas and soil CO_2 flux measurements were carried out for each station. Radon and thoron were measured using a Durridge RAD7 detector coupled with a steel probe, while soil CO_2 flux was measured using a West Systems LICOR-based portable CO_2 flux meter via accumulation chamber method. The survey grid covers an area of 7.20 km^2.

In some stations which correspond to surface expressions of the intercept of wells with faults, correlation between soil gases and fault permeability can be established using logistic regression. The general form of the logistic regression equation is:

$$P(y = 1|x_1, \dots x_i) = \frac{1}{1+e^{-(\beta_0+\beta_1 x_1+\cdots \beta_i x_i)}} \quad (1)$$

where $P(y = 1|x_1, \dots x_i)$ is the probability of desired outcome (*i.e.* dependent variable, y), $x_1 \dots x_i$ is the independent variable or predictor, β_0 is the coefficient of the intercept, and $\beta_1 \dots \beta_i$ is the coefficient of the predictor.

Based on evaluations of permeability from drilling, geology and completion tests, a value of "1" was set for stations positioned at intercepts with reported good permeability and "0" for stations located on intercepts with reported poor permeability. The input database for the model consists of the continuous variables (radon and thoron concentration, CO_2 flux), and the discrete variable (permeability). The desired outcome is to predict "highly permeable" areas based on soil gas concentration values measured at the surface, with the assumption that vertical permeability is continuous. By evaluating equation (1), a threshold value (x_i) for soil gas concentration and flux depicting highly permeable areas can be calculated. The derived value is used to assess the occurrence of structures with probable high permeability (Mismanos & Vasquez, 2015).

The interpolation of the gridded soil gas data to produce a 2D map was done using sequential Gaussian simulation (sGs). Threshold values derived from logistic regression results were then added to these maps for representing anomalous areas depicting the likely permeable structures.

3. RESULTS AND DISCUSSIONS

3.1 Logistic Regression Modelling

A total of 325 soil gas measurements were collected from the grid survey. Of these, 58 are located in well-fault intersections and are included in the logistic regression modelling. A summary of the database used for modelling is presented in Table 1.

Table 1: Summary of Database Used for Logistic Regression Modelling

Permeability *P*	*N*	Radon (Bq/m^3)	Thoron (Bq/m^3)	CO_2 Flux (g·m^{-2}·d^{-1})
Good (1)	33	2,045–45,167	974–21,000	5.47–33.5
Poor (0)	25	462–13,133	474–12,800	7.26–35.61

The results of the logistic regression are presented in Table 2 below. Model A, which predicts permeability based on radon and thoron only, is the most significant model. This model was selected because 1) each variable in the model were at least 95% significant, 2) it has the lowest AIC (Akaike Information Criterion) among the models, and 3) the model allows a good balance in sensitivity, specificity, and PCC (percent of correct classification). CO_2 flux, on the other hand, is only 90% significant, and therefore does not strongly support a correlation with permeability. The correlation of soil CO_2 flux with the other soil gases may be largely affected by biogenic sources of CO_2, especially since the survey areas are largely vegetated with rich organic content.

Table 2: Results of Logistic Regression Modelling

	Model	% Significance			null deviance	residual deviance	AIC	SE	SP	PCC	cutoff
		Rn	Tn	fCO_2							
A	P ~ Rn+Tn	99	95	-	79.3	64.9	70.9	0.70	0.68	0.69	0.52
B	P ~ Rn+Tn+fCO_2	99	99	90	79.3	64.5	72.5	0.67	0.68	0.67	0.55

The corresponding equation for Model A is shown in the equation below:

$$P = \frac{1}{1+e^{-[(-1.741)+1.333\times10^{-4}(\boldsymbol{Rn})+1.4567\times10^{-4}(\boldsymbol{Tn})]}} \quad (2)$$

Model A indicates that the permeability cutoff is 0.52. Using Equation 2, the permeability was solved for each station to obtain the distribution of permeability in the study area. In succeeding discussions, the computed thresholds will be used to identify anomalous degassing areas associated with highly permeable structures.

3.2 Soil Gas and Permeability Maps

The mapped soil gas concentrations (radon and thoron) are shown in Figure 2 below. In general, most of the radon concentration threshold contours occur at structures and structural intersections where wells have been drilled. The Okoy Fault and Cross Splay Fault appear to contain the considerable anomalies, suggesting a major structural control. The largest and perhaps the most important in this area is the large anomaly contour at Region A, straddling the northwest-oriented Okoy Fault and faults terminating on this structure. The Region A anomaly not only includes stations above the faults. There are numerous, adjacent off-fault stations occurring in this area, suggesting that this is indeed a major degassing zone. Although a major structure, the limited extent of anomaly along Okoy Fault implies that permeability may be confined on this segment only.

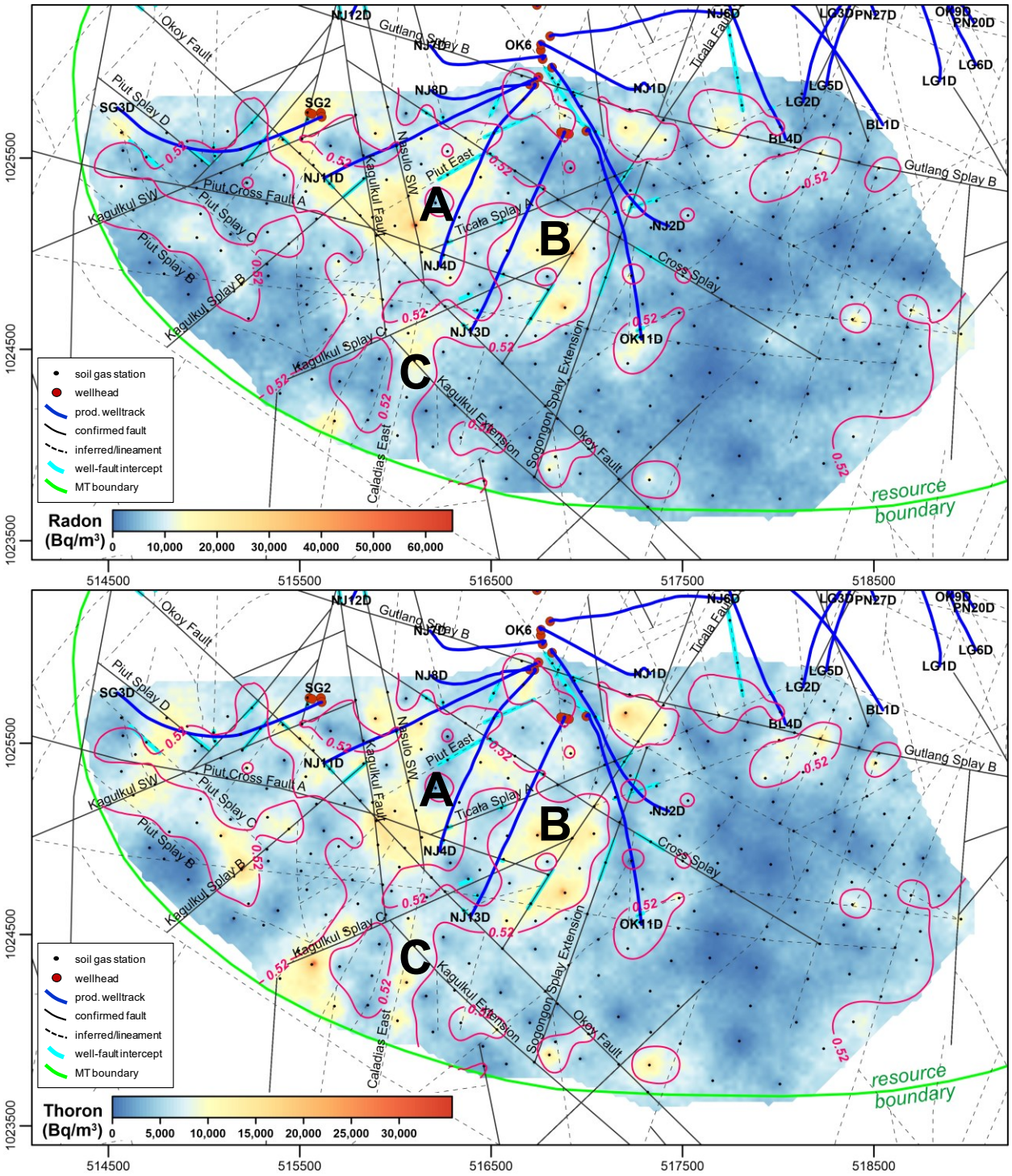

Figure 2: Radon (top) and thoron (bottom) anomaly maps showing permeability cutoff at 0.52.

Okoy Fault has the most pronounced and consistent anomaly beginning from its permeable zone with SG-3D to its intersection with the Nasulo SW terminus. Wells SG-2 and NJ-11 attribute their major permeable zones in this fault segment (Reyes & Hermoso, 2015), while NJ-13 was blind-drilled along this structure and has a two permeable zone in this fault (Tabios & Hermoso, 2015). Meanwhile, SG-3D is cased off in this section but experienced total circulation losses upon intersection with this fault (Seastres Jr., 1983b). The Kagulkul Splay B Fault, a portion of which is bounded by the anomaly, overlaps with Okoy Fault in its intersection with NJ-11D and can be conferred with the same characteristics.

The Cross Splay Fault appears to bound the northwest extent of the soil gas anomaly, suggesting a structural control on the degassing. Wells NJ-11D, NJ-13D, NJ-4D, and OK-11D intersected this fault and reported major and minor permeable zones, open fractures, and partial to total circulation losses (Reyes & Hermoso, 2015; Seastres Jr., 1981, 1983c; Tabios & Hermoso, 2015).

NNW-SSE oriented structures such as the parallel Nasulo SW and Kagulkul Faults host a major soil gas-permeability anomaly. Wells NJ-11D and NJ-12D encountered this fault and reported minor permeable zones (Reyes & Hermoso, 2015).

The trace of the Piut East Fault is also well within the anomaly. NJ-4D has a major permeable zone with this fault that is shared with Cross Splay because of their overlap. Drilling along this structure/s, NJ-4D encountered drusy quartz/anhydrite crystals, partial and total circulation losses which eventually resulted to blind drilling (Seastres Jr., 1983c).

Another major anomaly is Region B, occurring close to the terminus of northeast-trending Ticala Fault with Okoy Fault. This degassing zone involves the terminus of Kagulkul Splay C and Piut Cross Fault A. Downhole structural data from this zone is provided by NJ-13D. The Ticala Fault, Kagulkul Splay-C, Piut Cross Fault A, and Kaipohan Cross Faults are responsible for several minor permeable zones, although the major zone of NJ-13D was attributed to its intersection with Ticala Splay A (Tabios & Hermoso, 2015). For Ticala Fault, the well came across moderate to abundant vein minerals and experienced partial and total circulation losses. Inspite these indications, the well failed to sustain discharge and generally considered to be drilled into an impermeable section. It is difficult to consider a great chance of encountering good permeability in this area, given that the wells which bound Region B anomaly are not successful in tapping open fractures.

A sizeable anomaly occurs on the intersection of Kagulkul Fault, Kagulkul Splay C, and Kagulkul Extension, indicated herein as Region C. A portion of the anomaly touches the intercept of NJ-13D with Okoy Fault, which bore it a minor permeable zone. The shape of this anomaly considerably varies between radon and thoron.

Considerable segments of Piut Cross Fault A are also interpreted to be permeable. This has been proven in wells NJ-4D where it encountered blind drilling and minor permeable zone (Seastres Jr., 1983c), and NJ-13D (Tabios & Hermoso, 2015) which reported a major permeable zone. The Piut Splays provided the major permeable zones for SG-3D (Seastres Jr., 1983b). The high soil gas anomaly straddles these structures. Southwest of these structures, a parallel sizeable anomaly is also outlined. This indicates that the NW-SE faults act as structural controls to the degassing.

Several spot anomalies can be associated to the trace of Gutlang Splay B. This may also indicate a structurally controlled degassing along this fault. The absence or minimal occurrence of gas anomalies east of Nasuji (NJ wells) and south of Balas-Balas (BL wells) sector suggests that there is not much to expect in terms of structural permeability in this area. This is consistent with the poor permeability encountered by NJ-2D (Seastres Jr., 1983a) and OK-11D (Seastres Jr., 1981).

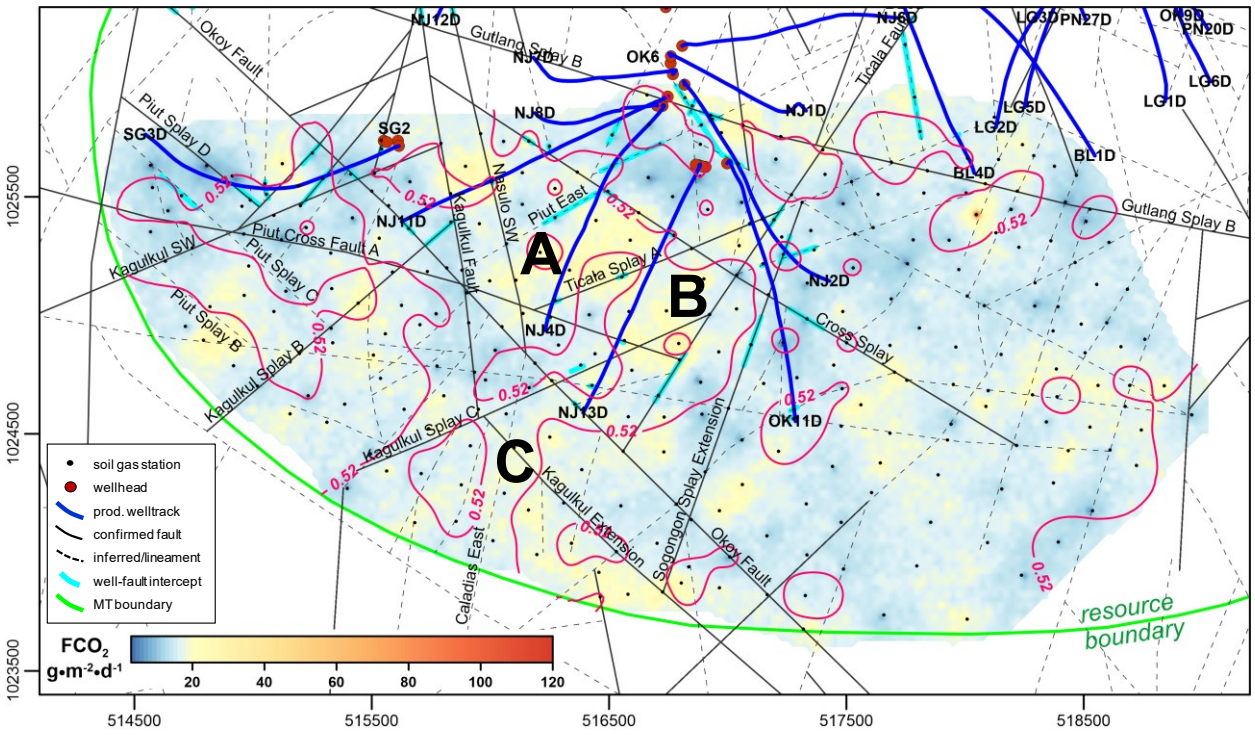

Figure 3: Soil CO2 flux distribution map, overlain with the permeability cutoff contour at 0.52

Figure 3 shows the distribution of CO2 flux in the study area. CO2 flux was not a significant factor in the logistic regression modeling, and its distribution throughout the field is quite indistinctive too. The region bounded by Ticala, Okoy, and Cross Splay Faults appear to host the elevated flux values. Patches of elevated flux, although limited in extent, are scattered around the study area and occur at or near faults or multiple fault intersections. Nevertheless, occurrence of anomalies by two or more gases strongly point to the degassing at these zones, despite the size of anomaly.

3.3 Permeable Structures

From the soil gas mapping, three sets of structures appear to be the permeable structural orientations. Figure 4 shows the map of permeability based on logistic regression, highlighting the permeability cutoff value of 0.52. Specifically, the following are the interpreted permeable faults:

1. NW-SE oriented structures: Gutlang Splay B Fault, Cross Splay Fault, Okoy Fault, Piut Splays
2. NNW-SSE oriented structures: Nasulo SW, Kagulkul Fault
3. NE-SW oriented structures: Kagulkul Splay D, Caladias East, Ticala Fault

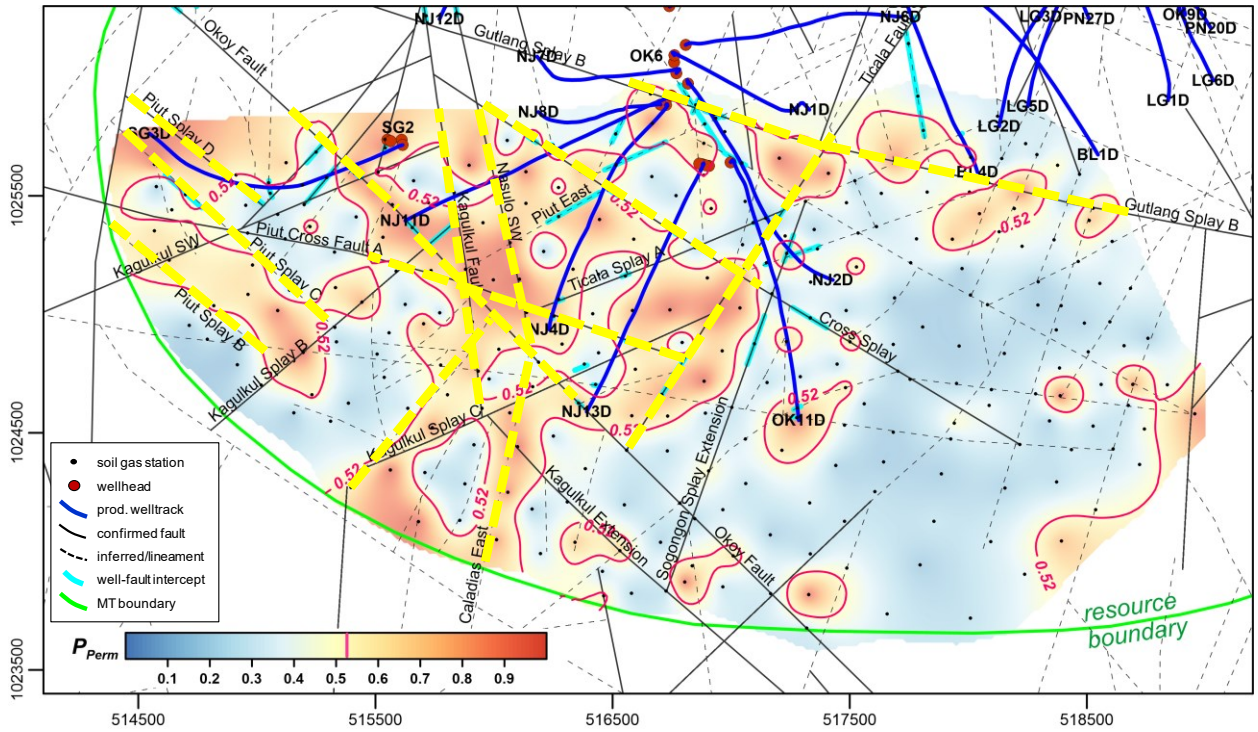

Figure 4: Permeability distribution map and the inferred permeable structures in South Sogongon and Nasuji

4. CONCLUSIONS

The soil gas survey conducted in Palinpinon Geothermal Field showed that soil gas anomalies can be correlated to the permeability characteristics of structures. The relationship between soil gases and permeability was modeled using logistic regression to obtain a threshold that can bound permeable structures. The best model was evaluated to have the relationship P ~ Rn + Tn, describing the probability that a structure is permeable when radon and thoron occur at high concentrations in soil gas.

The NW-SE and the NE-SW faults appear to bound the largest anomalies, and are also the major structures functioning as the major vertical permeable pathways for gases of deep origin in this area of the resource. These structures could be targeted by future drilling campaigns in search of sources of permeability. To be able to increase certainty and reduce risk in permeability exploration, soil gas data must be interpreted in conjunction with as much geoscientific and reservoir data as possible.

REFERENCES

Chiodini, G., Cioni, R., Guidi, M., Raco, B., & Marini, L. (1998). Soil CO2 flux measurements in volcanic and geothermal areas. *Applied Geochemistry*, *13*(5), 543–552. https://doi.org/10.1016/S0883-2927(97)00076-0

Cox, M. E. (1980). Ground radon survey of a geothermal area in Hawaii. *Geophysical Research Letters*, *7*(4), 283–286.

Klusman, R. W., Moore, J. N., & LeRoy, M. P. (2000). Potential for surface gas flux measurements in exploration and surface evaluation of geothermal resources. *Geothermics*, *29*(6), 637–670. https://doi.org/10.1016/S0375-6505(00)00036-5

Mahon, W. A. J., McDowell, G. D., & Finlayson, J. B. (1980). Carbon dioxide: Its role in geothermal systems. *New Zealand Journal of Science*, *23*, 133–148.

Mismanos, J., & Vasquez, A. (2015). *Repeat Soil Radon and CO2 Flux Survey in Mahanagdong, Leyte Geothermal Field* (p. 44) [Internal Report]. Pasig City: Energy Development Corporation.

Reyes, J. K., & Hermoso, D. (2015). *Geology of Well NJ-11D* (p. 344) [Internal Report]. Pasig City: Energy Development Corporation.

Seastres Jr., J. S. (1981). *Downhole Geological Summary of Okoy 11D* (p. 8) [Internal Report]. Makati City: PNOC-EDC.

Seastres Jr., J. S. (1983a). *Downhole Geology of Well NJ-2D* (p. 32) [Internal Report]. Makati City: PNOC-EDC.

Seastres Jr., J. S. (1983b). *Preliminary Downhole Geology of SG-3D* (p. 35) [Internal Report]. Makati City: PNOC-EDC.

Seastres Jr., J. S. (1983c). *Preliminary Geology of Well NJ-4D* (p. 56) [Internal Report]. Makati City: Energy Development Corporation.

Tabios, I., & Hermoso, D. (2015, September). *NJ13D Re-Interpreted Well-Fault Intersections*. Presented at the Valencia, Negros Oriental. Valencia, Negros Oriental.

Vasquez, A., Abecia, V. M., & Cariaga, C. (2015). *Soil Radon Gas Survey in Botong-Rangas Reinjection Area, Bacon-Manito Geothermal Project* (p. 54) [Internal Report]. Pasig City: Energy Development Corporation.

Voltattorni, N., & Lombardi, S. (2010). Soil gas geochemistry: Significance and application in geological prospectings. *Natural Gas*.

Werner, C., & Cardellini, C. (2006). Comparison of carbon dioxide emissions with fluid upflow, chemistry, and geologic structures at the Rotorua geothermal system, New Zealand. *Geothermics*, *35*(3), 221–238. https://doi.org/10.1016/j.geothermics.2006.02.006

Witcher, J. C. (1991). Radon soil-gas surveys with diffusion-model corrections in geothermal Exploration. *Geothermal Resources Council, Transactions*, *15*, 301–308.